J Mater Sci (2006) 41:5619–5624
DOI 10.1007/s10853-006-0261-y

Correlation between optical, electrical and structural properties of vanadium dioxide thin films

N. R. Mlyuka · R. T. Kivaisi

Received: 10 March 2005 / Accepted: 19 October 2005 / Published online: 20 June 2006
© Springer Science+Business Media, LLC 2006

Abstract VO_2 films have been prepared on normal microscope glass slides by reactive rf magnetron sputtering of vanadium target in a mixture of argon and oxygen. Optical properties of the films were investigated by the UV/Vis/NIR Perkin–Elmer Lamda 9. Transmission electron microscope and atomic force microscope were used to investigate the structure of the films. Correlation between structural and optical properties of VO_2 thin films is investigated with respect to the dependence of both to substrate temperature.

Introduction

Over four decades have passed now since Morin, 1959 [1], reported a phase transition in vanadium dioxide (VO_2) for the first time. The following years saw an intense growing interest on the material, both from scientific and application points of view [2–4]. Vanadium dioxide is a first order phase transition material that displays temperature dependent changes in structural, electrical and optical properties, making it lie in a large class of materials that show large temperature induced changes in optical properties; a property known as thermochromism.

VO_2 can reversibly change from semiconductor to metallic phase when its temperature is raised beyond a critical point τ_c, reported to be ~68 °C [4–7]. As such VO_2 films have a potential to be used as thermo switch in energy efficient windows. Thus for example, glass windows coated with vanadium dioxide film will transmit both the luminous and the heating components of the solar radiation at lower temperature, but will be almost opaque especially to the heating component of the solar radiation when its temperature is raised above the critical point.

For VO_2 films to be used for practical window applications, several requirements need to be satisfied. Some of these requirements are higher switching magnitude in the near infrared wavelengths; increased sharpness in switching, switching effectively at near room temperature and lowering thermal hysteresis width during switching.

In this paper we investigate the correlation between optical and electrical properties of VO_2 films with its structure in an attempt to optimize optical and electrical performance of the films.

Experimental procedure

VO_2 thin films were deposited on quartz glass slides by reactive magnetron sputtering method. A 50 mm water-cooled vanadium target (99.9% purity) was sputtered in an $Ar–O_2$ discharge to form oxide films. The rf power of 150 W and working pressure of about 3.8×10^{-3} was maintained. Gas flow meters controlled precisely the flow rates of oxygen and argon at about 1.4–3.0 and 76 ml/min respectively. A radiant heater was used to heat the samples to between 250 and 400 °C. These deposition conditions were comparable to those from an earlier work [8] and that done by Jin et al. [7]. Both produced stoichiometric VO_2 films as observed by X-ray Diffraction (XRD) and Rutherford Backscattering Spectroscopy (RBS). Samples for microstructure analysis in the transmission electron

N. R. Mlyuka (✉) · R. T. Kivaisi
Solar Energy Group, Physics Department, University of Dar es salaam, Uvumbuzi Road, P. O. Box 35063, Dar es salaam +255, TANZANIA
e-mail: nmlyuka@yahoo.com

microscope was sputtered onto 3 mm carbon covered copper grids simultaneously with those on quartz glass slides. Carbon covered copper grids were used because they have good electrical properties, high transparency to electrons and good stability when placed under the electron beam.

The optical transmittance measurements were made near normal incidence using Perkin–Elmer Lambda 9 (UV–Vis–NIR). Wavelength dependence transmitance was measured in the range 300–2,500 nm at constant temperatures of 20 and 100 °C corresponding to semiconductor and metallic states of VO_2 films. Transmittance as a function of temperature taken at 2,500 nm, a wavelength at which most of the samples show the largest contrast in transmittance on switching, was recorded. A critical temperature, τ_c, was obtained at the mid-point of the transmittance–temperature curve during cooling.

Sheet resistance of the films as a function of temperature was measured by two point-probe method in the temperature range of 20–120 °C corresponding to semiconductor and metallic phases of the films.

The surface morphology characterization was done by a Digital Instruments Nanoscope IIIa Multimode Atomic Force Microscope in tapping mode.

A roughness (R_a) value was defined as the mean value of the surface relative to the central plane,

$$R_a = \frac{1}{L_x L_y} \sum_{0}^{L_y} \sum_{0}^{L_x} [f(x, y)] \mathrm{d}x\mathrm{d}y$$

where $f(x,y)$ is the surface relative to the central plane and L_x and L_y are the dimensions of the surface.

Bulk, structural analysis was performed using the LEO 910 analytical transmission electron microscope (TEM). Diffraction patterns from the TEM were used to judge the order of crystallinity of the films.

It was not possible to perform structural characterization at high temperature phase because of lack of heating facility in the electron microscope and the atomic force microscope.

The Quartz Crystal Thickness Monitor incorporated in the sputtering unit was used to monitor film thickness during deposition. Time durations used to achieve several sets of film thickness was recorded during monitoring deposition. These time periods were then used to estimate thickness of samples deposited under high temperature.

Results and discussion

Optical properties

Films deposited at 350 °C showed the best switching behaviour. Figure 1 shows a graph of transmittance against temperature at $\lambda = 2500$ nm, the wavelength at which the sharpest contrast is observed between the two temperature phases. It was observed that samples deposited at 350 and 400 °C had curves with sharp knee especially during cooling. Samples deposited at 250 and 300 °C however showed weak thermochromism, where the difference in transmittance ΔT between the high and low temperature phases is small.

The curves in Fig. 1 showed an increase of ΔT with increase in deposition temperature, from $\Delta T < 10\%$ for samples deposited at 250 °C to $\Delta T > 50\%$ for samples deposited at 350 °C. Hysteresis width of the films deposited at higher substrate temperature was found to be thinner than that for films deposited at low temperature.

For bulk VO_2, the transition temperature occurs at ~67 °C with a narrow switching interval (between transparency and opaque) of 0.1 °C and a thermal hysteresis width of 1.4 °C [4, 9]. For thin films on the other hand it is difficult to apply the concept of transition temperature because transition usually occurs at fairly wide temperature intervals and relatively wider hysteresis width [10].

Even though, an effective phase transition temperature proposed by Begishev et al. [9] defined as either the temperature at the mid point at the transmittance–temperature (T–τ) curve on the heating portion, or more exactly, as the maximum of the derivative of the temperature dependence of transmittance, i.e., $\mathrm{d}T(\tau)/\mathrm{d}\tau$, was used to evaluate the phase transition of VO_2 films, as has been done by many authors [7, 8, 11].

The transition temperature was found to be 68 °C, which is in a good agreement with that reported elsewhere [2, 7] and also consistent with the value for bulk VO_2 [12].

Electrical properties

The change in resistivity with temperature for VO_2 films deposited under different substrate temperatures is shown

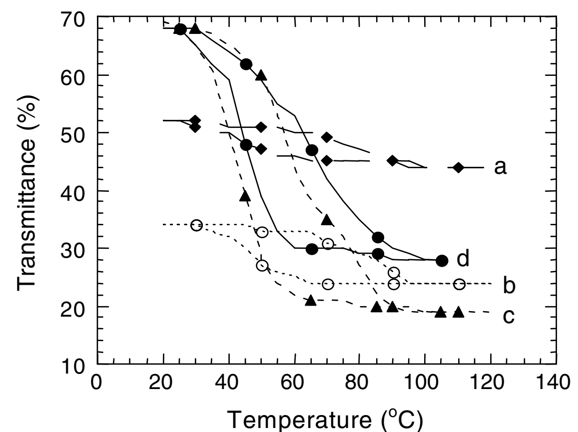

Fig. 1 Temperature dependence of transmittance at 2,500 nm for ~1,000 Å VO_2 films deposited at (**a**) 250 °C (**b**) 300 °C (**c**) 350 °C and (**d**) 400 °C.

in Fig. 2. Sheet resistance of the films showed strong dependence to the deposition temperature. Samples deposited at 350 °C showed the highest ratio of resistivity, ~10^3, between the semiconductor and metallic phases of the films, a value corresponding well with that reported by other authors [5, 7, 13, 14]. The films show (Fig. 3) a sharper resistivity change close to the transition temperature. At 300 °C the ratio was only one order of magnitude with gentler slope close to transition temperature, where as those deposited at 250 °C had resistivity ratio of less than an order of magnitude (Fig. 2).

Structural properties

Transmission Electron Microscopy of VO_2 thin films revealed a marked dependence of the film structure on the deposition temperature, T_s. The TEM microstructure of films deposited at 250 and 300 °C showed very small grains, less dense surfaces with a lot of voids through the surfaces (Figs. 4a, 5a). The micrograph of the film deposited at ~350 °C (Fig. 6a) showed well-crystallized grains with mean diameter of ~25 nm. The grains were faceted with grain boundaries of about 5.5 nm. For films deposited at T_s~400 °C, the grains seemed to have agglometed, forming almost a continuous film (Fig. 7a). For all the films there were no indication of any ordered structural defect, which suggests that the films were homogeneous.

The electron diffraction patterns for samples deposited at 250 and 300 °C showed spotted ring patterns (Figs. 4b, 5b) that suggest development of regions of localized crystallinity. For the films deposited at 350 and 400 °C, Fig. 6b, 7b, the diffraction patterns are very ordered symmetrical spot patterns typical of single-crystal VO_2.

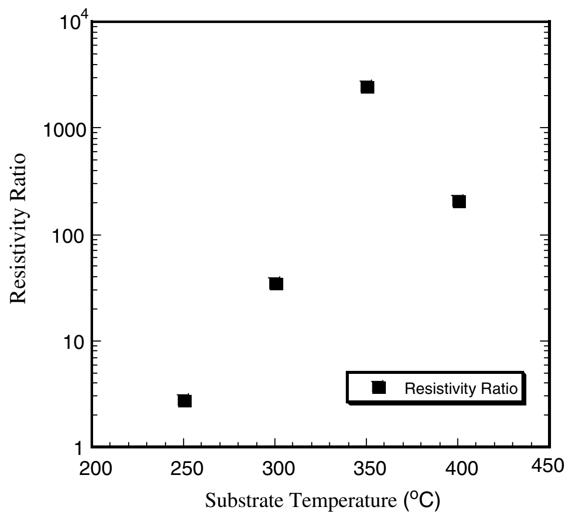

Fig. 2 Resistivity ratios of VO_2 films deposited at different substrate temperature

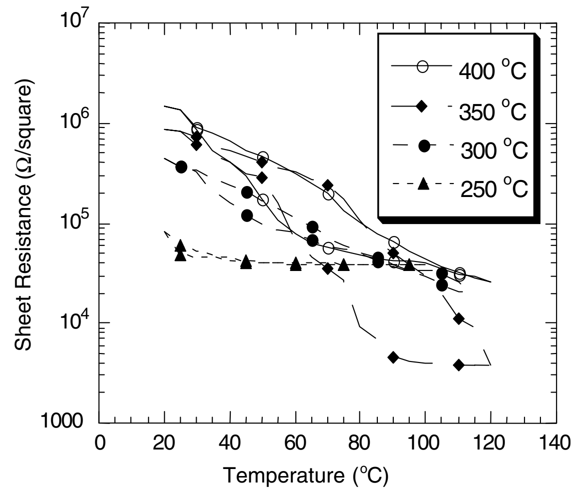

Fig. 3 Sheet resistance versus temperature for VO_2 films deposited at 250, 300, 350, 400 °C.

AFM images of VO_2 films revealed strong dependence of the surface morphology and grain formation on the substrate temperature. The morphological change corresponding to the evolution of crystallization is observed in these AFM images. The images of samples deposited at 250 and 300 °C correspond well with the TEM microstructure, the surfaces were less dense with spacey grains of mean (lateral area) sizes of ~115 and ~946 nm^2 respectively. The surface roughness (R_a) was found to be 5.36 and 2.6 nm respectively for samples deposited at 250 and 300 °C (Figs. 8a, 9a). Figures 8b, 9b show the cross sections of the films deposited at 250 and 300 °C, the sections revealed maximum peaks (of grains) of 13.8 and 10.8 nm respectively.

Figures 10, 11 show AFM micrographs and cross-section for films deposited at 350 and 400 °C respectively. At 350 °C the film has large tall forest of grains of mean size 1,431 nm^2 with mean roughness (R_a) of 5.2 nm. Maximum cross sectional (grain) height is ~37.3 nm. At 400 °C the grains seem to have coalesced forming larger grain clusters about semi-spherical with mean grain size of 5,840 nm^2 and roughness of 5.0 nm. There is a positive evolution of grains with increasing substrate temperature. These results are supported by other authors [15, 16].

Deposition temperature of 250 °C for VO_2 lies in the region with $T_s/T_m < 0.3$ which lies in zone 1 of the Thorntons Model of film structure growth (melting temperature for VO_2 is 1800 K [17]), this zone is characterized by small grains with many voids in the film. A sharp jump in grain size is observed at 400 °C, this temperature lies in the range $T/T_m = 0.5$ wich is zone 2 of the Thorntons Model, a zone at which the grains penetrate through the whole thickness of the films, forming large and sometimes

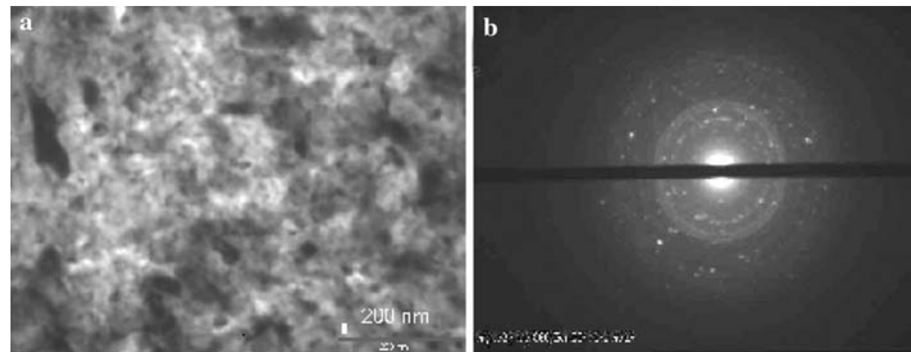

Fig. 4 TEM micrograph (**a**) and electron diffraction image (**b**) of VO_2 film deposited at 250 °C

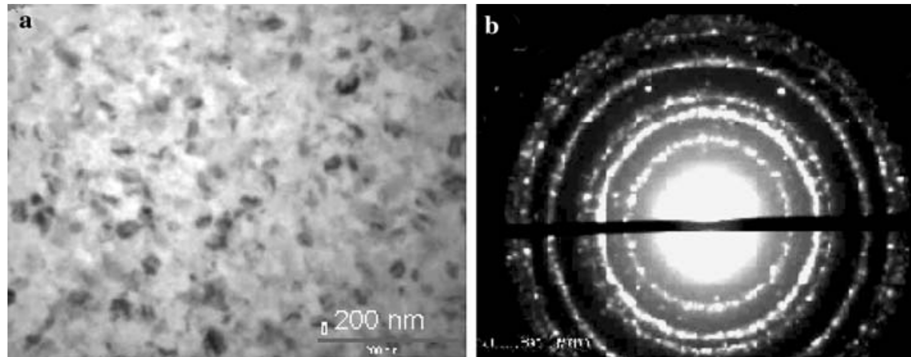

Fig. 5 TEM micrograph (**a**) and electron diffraction image (**b**) of VO_2 film deposited at 300 °C

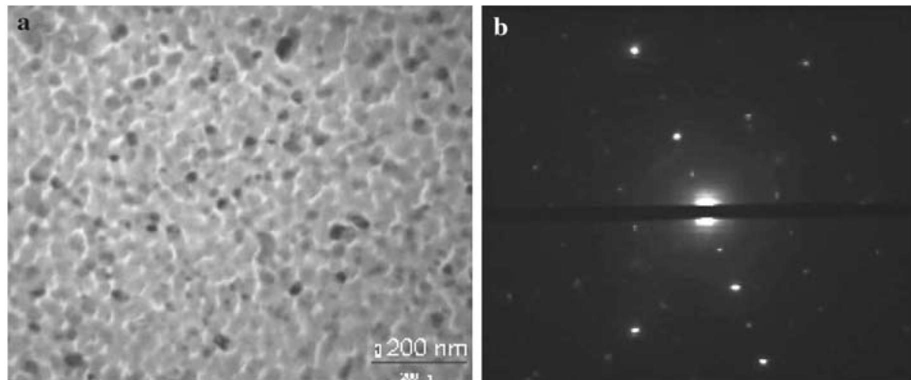

Fig. 6 TEM micrograph (**a**) and electron diffraction image (**b**) of VO_2 film deposited at 350 °C

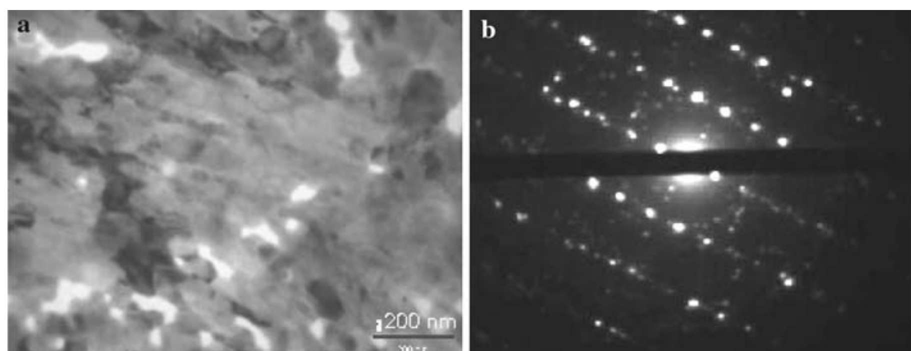

Fig. 7 TEM micrograph (**a**) and electron diffraction image (**b**) of VO_2 film deposited at 400 °C

columnar grains. At this temperature grain boundary migration and recrystallization within grains is dominant [18–20]. This leads to fewer crystal defects and better crystallinity as the AFM and also TEM results show.

It has been argued that optical transition is controlled by the number of individual grains that has transformed, where as resistance change is strongly dependent upon the nature of the grain boundary structures and percolation

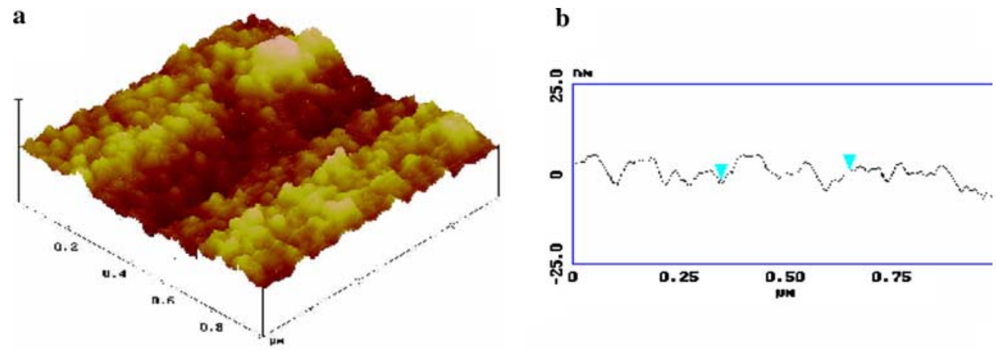

Fig. 8 AFM image (**a**) and cross-section (**b**) of VO_2 film deposited at 250 °C.

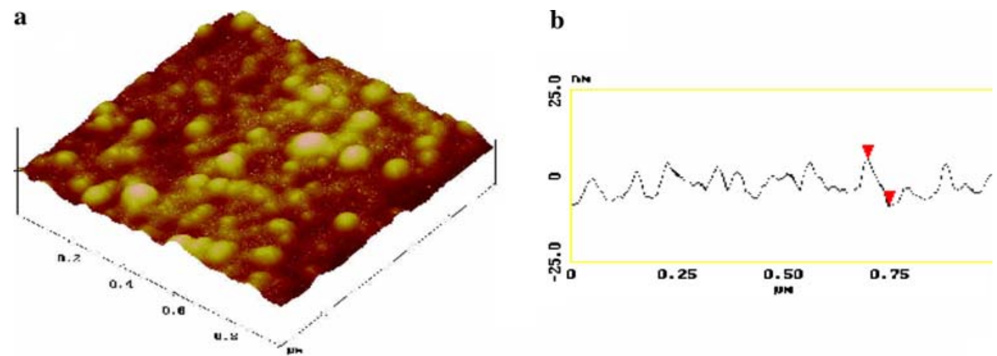

Fig. 9 AFM image (**a**) and cross-section (**b**) of VO_2 film deposited at 300 °C

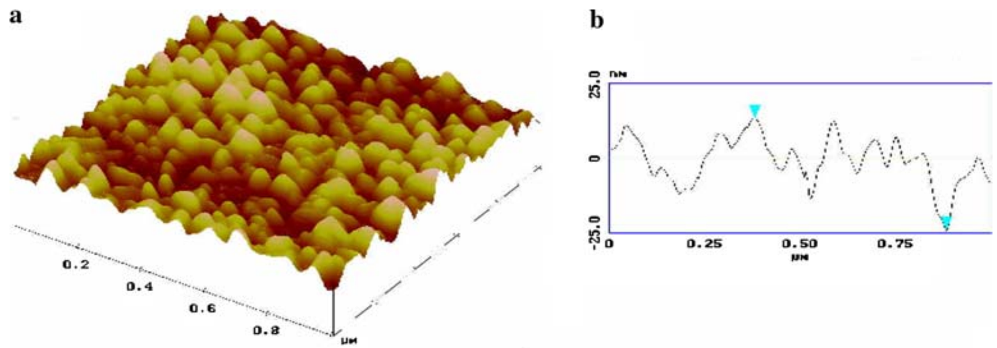

Fig. 10 AFM image (**a**) and cross-section (**b**) of VO_2 film deposited at 350 °C

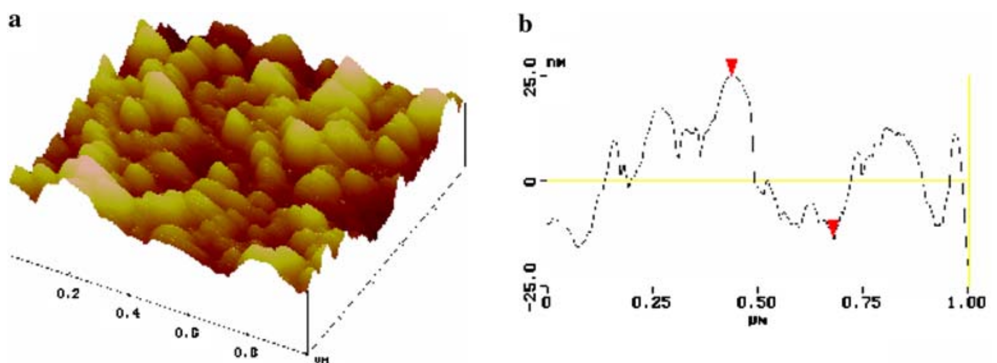

Fig. 11 AFM image (**a**) and cross-section (**b**) of VO_2 film deposited at 400 °C

effects [13, 21]. As the results indicate, decrease in T_s result in a significant decrease in crystallite size and vice versa. The reduction in crystallite size increases crystal imperfections, that include the number of atoms distributed randomly near the crystallite boundaries at which the ordered zigzag chains of the V–V pairs characteristic of the low temperature phase are destroyed, leading to the destabilization of the semiconductor phase and the decrease in τ_c and also the transition sharpness [7]. This has been demonstrated in our results.

Conclusions

Deposition temperature was found to have great influence on the structure growth of VO_2 thin films. Higher deposition temperatures resulted in films with better crystallinity. Growth of the films was found to fit well with Thorntons film growth model.

The study found a very strong dependence on optical and electrical properties to the structure of the films. The films with larger grain sizes and smaller surface roughness as determined by the AFM revealed better thermochromism. These films were observed to be rather continuous, with diffraction patterns taken within single grains showing very orderly spots arrangement like those in single crystals.

Acknowledgment Mlyuka, N. R. would like to thank the University of Dar es Salaam for scholarship. IPPS, Uppsala University, Sweden is also acknowledge for support including research equipment and materials.

References

1. Morin FJ, (1959) Phys Rev Lett 3:34
2. Sobhan MA, Kivaisi RT, Stjerna B, Granqvist CG, (1996) Sol Energy Mater Sol Cells 44:451
3. Granqvist CG (1991) In: Granqvist CG (ed) Energy efficient windows: present and forthcoming technology, Pergamon, Oxford
4. Ilinski A, Silva-Andrade F, Shadrin E, Klimov V, (2004) J Non-Cryst Solids 338(340):266
5. Babulanam SM, Eriksson TS, Niklasson GA, Granqvist CG, (1986) SPIE 692:007
6. Petit C, Frigerio J, Goldman M, (1999) J Phy: Condens Matter 11:3259
7. Jin P, Yoshimura K, Tanemura S, (1997) J Vac Sci Technol A 15(3):1113
8. Sobhan MA, Kivaisi RT, Stjerna B, Granqvist CG, (1994) SPIE 2255:423
9. Begishev AR, Galiev GB, Ignat'ev AS, Mokerov VG, Poshin VG, (1978) Sov Phys Solid State 20(6):951
10. Burkhardt BW, Christmann T, Franke S, Kriegseis W, Meister D, Meyer BK, Niessner W, Schalch D, Scharmann A, (2002) Thin Solid Films 402:226
11. Samiji ME (1997) Preparation and characterization of vanadium dioxide films M.Sc. Dissertation, University of Dar es salaam
12. Stephanovich G, Pergament A, Stephanovich D, (2000) J Phys Condens Matter 12:8837
13. Denatale JF, Hood PJ, Harker AB. (1989) J Appl Phys 66(12):5844
14. Roach WR, (1971) Appl Phys Lett 19(11):453
15. Buhling B, Michalowski L, (1976) LE VIDE 185:185
16. Cui J, Da D, Jiang W, (1998) Appl Surface Sci 133:225
17. Kusano E, Theil JA, (1989) J Vac Sci Technol A 7(3):1314
18. Thornton JA, (1974) J Vac Sci Tech 11(4):666
19. Thornton JA, (1975) J Vac Sci Tech 12(4):830
20. Thornton JA, (1986) J Vac Sci Tech A 4(6):359
21. Ambia MG, Islam MN, Hakim MO, (1992) Sol Energy Mater Solar Cells 28(2):103